# Electronic Supplementary Information

# A new photoelectrochemical biosensor for ultrasensitive determination of nucleic acid based on three-stage cascade signal amplification strategy

Erhu Xiong, Xiaoxia Yan, Xiaohua Zhang,* Yanmei Li, Ruiying Yang, Leixia Meng and Jinhua Chen*

*State Key Laboratory of Chemo/Biosensing and Chemometrics, College of Chemistry and Chemical Engineering, Hunan University, Changsha, 410082, P. R. China*

## Table of contents



*Corresponding author. Tel.: +86-731-88821961
E-mail address: chenjinhua@hnu.edu.cn; mickyxie@hnu.edu.cn

**(1) Sequences of oligonucleotides**

**Table S1.** Sequences of oligonucleotides used in this work[a]

| Oligonucleotides | Sequences (from 5' to 3') |
|---|---|
| C−DNA | HS−$(CH_2)_6$−CCCAATTTCCACCT |
| CHA−HP1 | *CTCCCCGA*CCCAATTTCCACCTTCGGGAGGGAA<br>AAGATGCTATGCGAT CGAAGGTGGAAATTGGG |
| CHA−HP2 | TCGATCGCATAGCATCTTTTCCCTCCCGAAGGTG<br>GAAATTGGGTCGG GGAGGGAAAAGATGCTCAT |
| HCR−HP1 | Biotin−GATGCTCATTGGTGTATGAGCATCTTTTCC−Biotin |
| HCR−HP2 | Biotin−ACACCAATGAGCATCGGAAAAGATGCTCAT−Bioti<br>n |
| T–DNA | *CGAAGGTGGAAATTGGGTCGGGGAG* |
| Sm–DNA | CGAAGGTGGACATTGGGTCGGGGAG |
| Tm–DNA | CGAATGTGGACATTGGGTCAGGGAG |
| N–DNA | TCGCACGGCTCATGACCTACAGAGCTCA |

[a]Abbreviation: capture DNA (C–DNA), catalytic hairpin assembly (CHA), hybridization chain reaction (HCR), hairpin (HP), target DNA (T–DNA), single–base mismatched DNA (Sm–DNA), three–bases mismatched DNA (Tm–DNA), and non–complementary DNA (N–DNA). The sequences in the same color in different oligonucleotides are complementary and the underlined sequences in the same oligonucleotide are complementary. The T–DNA in italics and the CHA−HP1 in italics are complementary.

**(2) TEM images of pure $TiO_2$ and $TiO_2$/CdS:Mn**

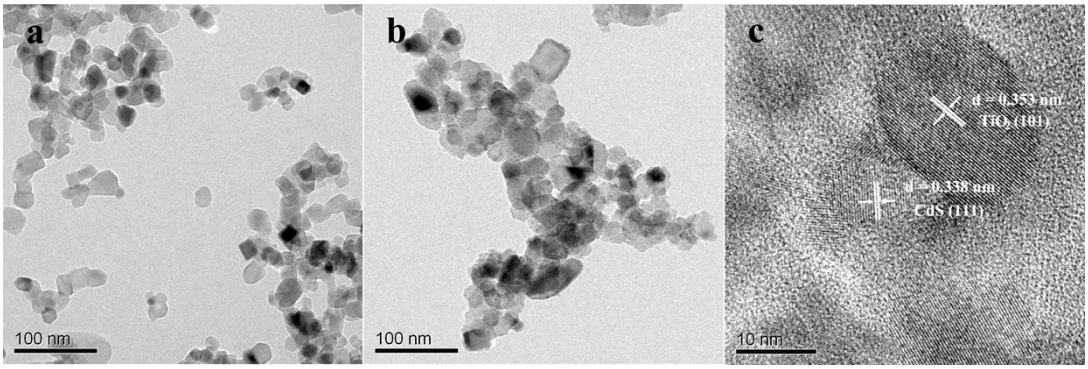


**Fig. S1** TEM images of (a) pure $TiO_2$ and (b) $TiO_2$/CdS:Mn, HRTEM image of (c) $TiO_2$/CdS:Mn.

**(3) EDS mapping of ITO/$TiO_2$/CdS:Mn sample**

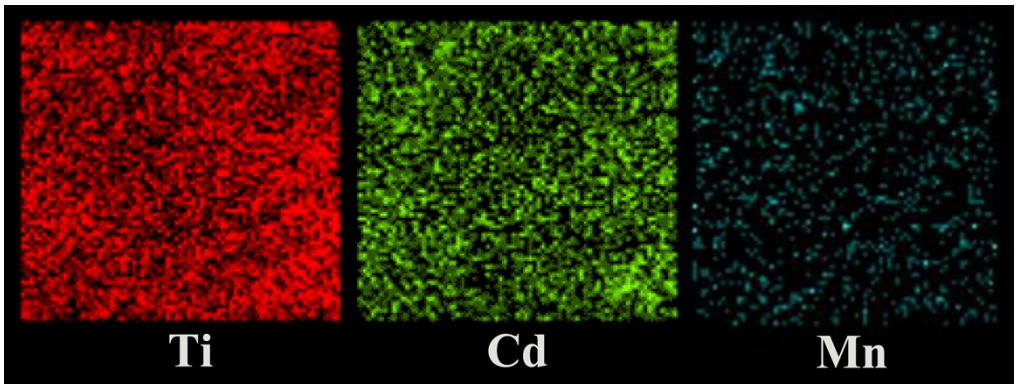


**Fig. S2** EDS mapping of ITO/$TiO_2$/CdS:Mn sample.

**(4) XRD patterns of $TiO_2$, $TiO_2$/CdS, and $TiO_2$/CdS:Mn**

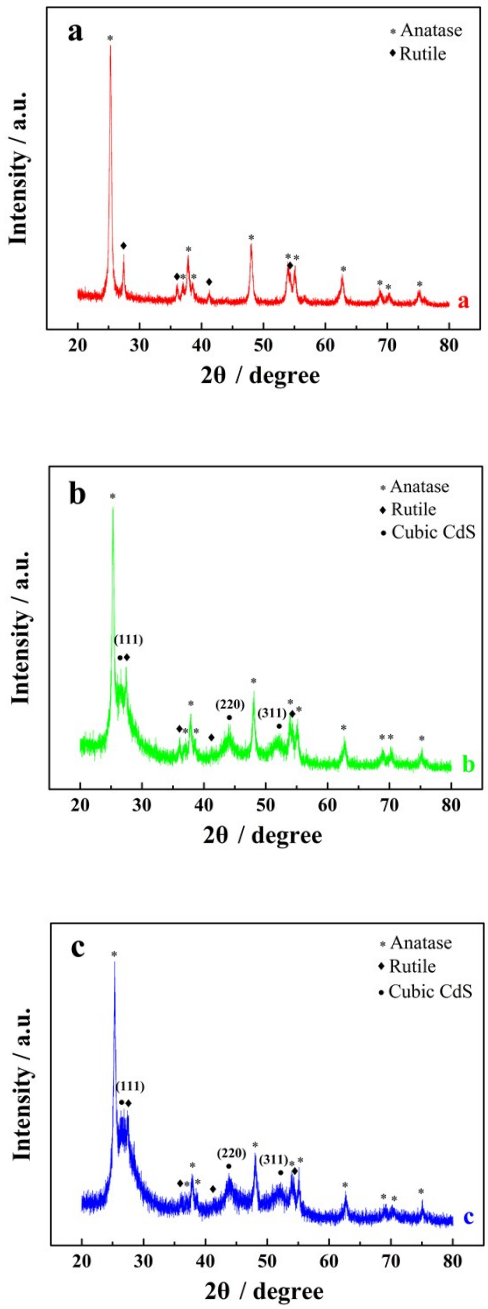


**Fig. S3** XRD patterns of $TiO_2$ (a), $TiO_2$/CdS (b), and $TiO_2$/CdS:Mn (c) samples.

All of these patterns show the same peaks at 25.32°, 37.0°, 37.79°, 38.58°, 48.03°, 53.93°, 55.11°, 62.71°, 68.87°, 70.31°, and 75.03°, corresponding to the diffractions from the (101), (103), (004), (112), (200), (105), (211), (204), (116), (220), and (215)

planes of anatase $TiO_2$ (JCPDS no. 21−1272); and other peaks at 27.42°, 36.08°, 41.19°, and 54.32° correspond to the diffractions from the (110), (101), (111), and (211) planes of rutile $TiO_2$ (JCPDS no. 21−1276). Besides, three characteristic peaks are observed at 26.51°, 44.08°, and 52.22° in Figures S3B and S3C, which correspond to the diffractions of the (111), (220), and (311) planes of CdS cubic structure (JCPDS no. 80−0019).

**(5) The role of AA on the PEC response of the FPEC electrode**

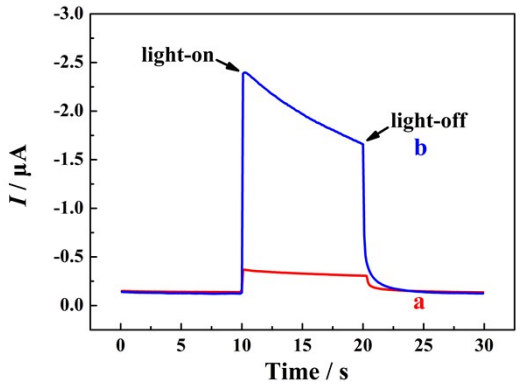


**Fig. S4** Photocurrent responses of the FPEC electrode in 10 mM Tris-HCl solution (pH 9.8) without AAP. Applied potential, −0.3 V; T–DNA, 20 nM. (a) without AA, (b) with AA (1 mM).

**(6) Optimization of the experimental conditions**

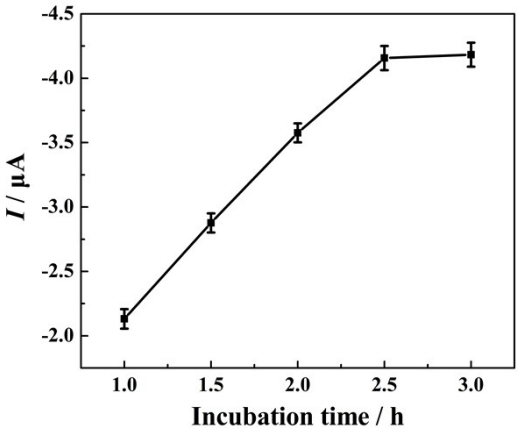


**Fig. S5** Incubation time for CHA process. The photocurrent intensity of the FPEC electrode was obtained in 10 mM Tris-HCl solution (pH 9.8) containing 0.1 mM $Mg(NO_3)_2$ and 20 nM T–DNA. Applied potential, −0.3 V; C−DNA concentration, 1.5 μM; AAP concentration, 10 mM; SA−ALP concentration, 0.1 mg/mL; the catalysis reaction time between ALP and AAP, 1.5 h. Error bars represent the standard deviation of three parallel experiments.

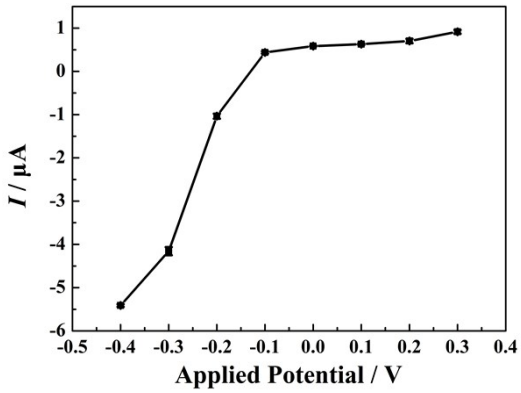


**Fig. S6** Influence of applied potential. The photocurrent intensity of the FPEC electrode was obtained in 10 mM Tris-HCl solution (pH 9.8) containing 0.1 mM $Mg(NO_3)_2$ and 20 nM T–DNA. Incubation time for CHA process, 2.5 h; C−DNA concentration, 1.5 μM; AAP concentration, 10 mM; SA−ALP concentration, 0.1

mg/mL; the catalysis reaction time between ALP and AAP, 1.5 h. Error bars represent the standard deviation of three parallel experiments.

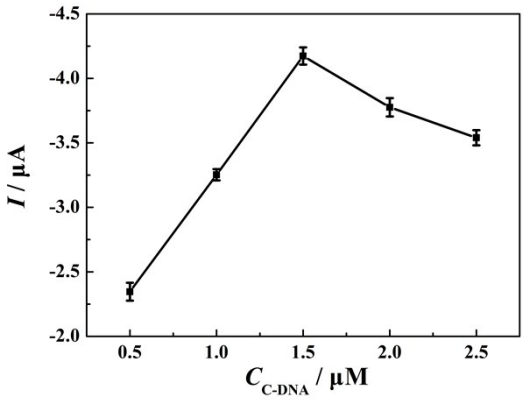


**Fig. S7** Influence of C−DNA concentration. The photocurrent intensity of the FPEC electrode was obtained in 10 mM Tris-HCl solution (pH 9.8) containing 0.1 mM $Mg(NO_3)_2$ and 20 nM T–DNA. Incubation time for CHA process, 2.5 h; Applied potential, −0.3 V; AAP concentration, 10 mM; SA−ALP concentration, 0.1 mg/mL; the catalysis reaction time between ALP and AAP, 1.5 h. Error bars represent the standard deviation of three parallel experiments.

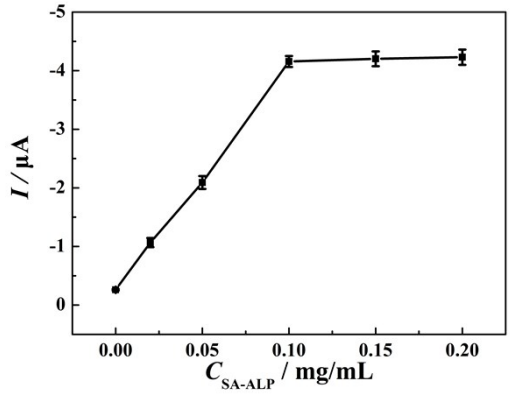


**Fig. S8** Influence of SA−ALP concentration. The photocurrent intensity of the FPEC electrode was obtained in 10 mM Tris-HCl solution (pH 9.8) containing 0.1 mM $Mg(NO_3)_2$ and 20 nM T–DNA. Incubation time for CHA process, 2.5 h; Applied

potential, −0.3 V; C−DNA concentration, 1.5 μM; AAP concentration, 10 mM; the catalysis reaction time between ALP and AAP, 1.5 h. Error bars represent the standard deviation of three parallel experiments.

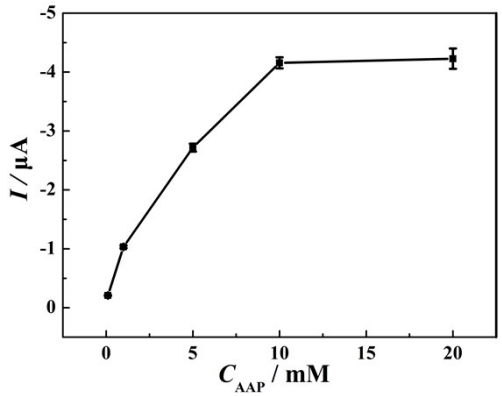


**Fig. S9** Influence of AAP concentration. The photocurrent intensity of the FPEC electrode was obtained in 10 mM Tris-HCl solution (pH 9.8) containing 0.1 mM $Mg(NO_3)_2$ and 20 nM T–DNA. Incubation time for CHA process, 2.5 h; Applied potential, −0.3 V; C−DNA concentration, 1.5 μM; SA−ALP concentration, 0.1 mg/mL; the catalysis reaction time between ALP and AAP, 1.5 h. Error bars represent the standard deviation of three parallel experiments.

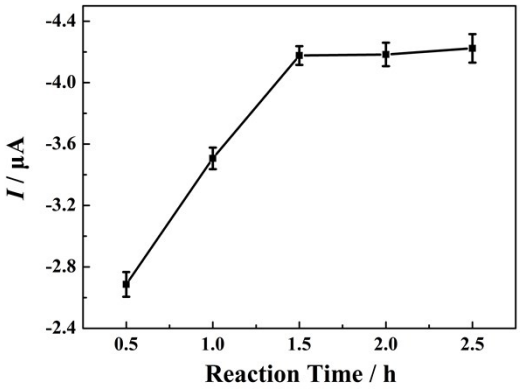


**Fig. S10** Influence of the catalysis reaction time between ALP and AAP. The photocurrent intensity of the FPEC electrode was obtained in 10 mM Tris-HCl

solution (pH 9.8) containing 0.1 mM $Mg(NO_3)_2$ and 20 nM T–DNA. Incubation time for CHA process, 2.5 h; Applied potential, −0.3 V; C−DNA concentration, 1.5 μM; AAP concentration, 10 mM; SA−ALP concentration, 0.1 mg/mL. Error bars represent the standard deviation of three parallel experiments.

**(7) Comparison of various analytical methods for DNA detection**

**Table S2.** Comparison of various analytical methods for DNA detection

| Analytical methods | Linear range | Detection limit | Reference |
|---|---|---|---|
| Electrochemiluminescence | 10 fM−0.5 nM | 1.4 fM | 1 |
| Electrochemiluminescence | 0.1 pM−10 nM | 0.1 pM | 2 |
| Electrochemistry | 1 fM−1 nM | 0.43 fM | 3 |
| Electrochemistry | 1 pM−100 nM | 0.9 pM | 4 |
| Colormetry | 10 fM−50 pM | 2.6 fM | 5 |
| Colormetry | 50 fM−35 pM | 50 fM | 6 |
| Fluorescence | 10 pM−100 pM | 10 pM | 7 |
| Fluorescence | 0.5 nM−140 nM | 0.29 nM | 8 |
| PEC | 5 fM−10 pM | 2.2 fM | 9 |
| PEC | 0.1 fM−100 pM | 0.052 fM | This work |

## References


1 F. Y. Zhou, H. Hai, Y. L. Yuan, P. J. Li, *Electroanal.*, 2017, **29**, 983–989.

2 M. Jiao, G. F. Jie, L. Tan, S. Y. Niu, *Anal. Chim. Acta*, 2017, **983**, 166–172.

3 G. Y. Zhang, S. Y. Deng, W. R. Cai, S. Cosnier, X. J. Zhang, D. Shan, *Anal. Chem.*, 2015, **87**, 9093–9100.

4 E. H. Xiong, Z. Z. Li, X. H. Zhang, J. W. Zhou, X. X. Yan, Y. Q. Liu, J. H. Chen, *Anal. Chem.*, 2017, **89**, 8830–8835.

5 Y. H. Guo, J. Wu, J. Li, H. X. Ju, *Biosens. Bioelectron.*, 2016, **78**, 267–273.

6 L. Chang, Y. Khan, L. D. Li, N. Yang, P. G. Yin, L. Guo, *RSC Adv.*, 2017, **7**, 13896–13903.

7 J. H. Huang, X. F. Su, Z. G. Li, *Anal. Chem.*, 2012, **84**, 5939–5443.

8 Y. H. Guo, Q. M. Chen, Y. T. Qi, Y. F. Xie, H. Qian, W. R. Yao, R. J. Pei, *Biosens. Bioelectron.*, 2017, **87**, 320–324.

9 Y. Zang, J. P. Lei, P. H. Ling, H. X. Ju, *Anal. Chem.*, 2015, **87**, 5430–5436.